Pharmacokinetic Comparison of Direct Antibody Targeting with Pretargeting Protocols Based on Streptavidin-Biotin Binding

Cynthia Sung and William W. van Osdol

Biomedical Engineering and Instrumentation Program, National Center for Research Resources, National Institutes of Health, Bethesda, Maryland; and Hybritech, Inc., San Diego, California

Several groups are currently investigating antibody pretargeting as a strategy for improving radionuclide delivery. Pharmacokinetic modeling of these protocols permits analysis of pretargeting protocols under a broad range of possible experimental conditions. **Methods:** We used previously developed pharmacokinetic models to predict the temporal uptake and spatial distribution of directly radiolabeled MAb, radiolabeled biotin given after pretargeting with streptavidinylated MAb and radiolabeled streptavidin given after pretargeting with biotinylated MAb in a microscopic, prevascular tumor nodule. Two dose regimens were investigated, as were the effects of internalization and degradation of antibody-antigen complexes (24-hr time constant). **Results:** Simulations indicate that the protocol involving streptavidinylated MAb and radiolabeled biotin yields higher tumor-to-blood and tumor-to-lung ratios and relative exposures than the other protocols. In the absence of antigen internalization, the peak average molar concentration and MRT of biotin in the tumor nodule is comparable to that of directly radiolabeled MAb, and the spatial distribution of radionuclide is more uniform. When antigen internalization occurs, the peak average concentration and the MRT in the tumor nodule are lower than the corresponding values for directly radiolabeled MAb. **Conclusion:** In the absence of antigen internalization, the protocol involving streptavidinylated MAb and radiolabeled biotin offers pharmacokinetic advantages over the other two protocols.

Key Words: pharmacokinetics; monoclonal antibodies; streptavidin; biotin; pretargeting

J Nucl Med 1995; 36:867–876

Pretargeting protocols seek to improve the diagnostic and therapeutic utility of MAbs by separating, in time, the function of antigen recognition from that of radionuclide localization (*1–8*). Such protocols require the use of a modified MAb that permits a second component to bind specifically to it. Conceptually, the modified MAb is administered first and is allowed to distribute throughout the body, to bind to the tissues expressing the antigen, and to clear substantially from other tissues. Then the radiolabeled second component is administered and, ideally, it localizes at sites where the modified MAb has accumulated. If the second component has higher permeation, clearance and diffusion rates than those of the MAb, more rapid radionuclide localization to the tumor and higher tumor selectivity are possible.

In this article, we compare, by the use of pharmacokinetic simulations, three different methods for specific tumor localization of a radionuclide. The methods are: (1) injection of a MAb directly labeled with a radionuclide; (2) injection of radiolabeled streptavidin (sAv) at a time, t_2, after injection of a biotinylated antibody (MAb-b); and (3) injection of radiolabeled biotin at a time, t_2, after injection of a streptavidinylated antibody (MAb-sAv). The simulations are performed using published pharmacokinetic models (*9–11*). Previous simulations with those models used parameter values that represented different organisms and normal tissues; hence, clear comparisons among the protocols were difficult to make. Here, all three protocols are evaluated using a consistent set of parameter values representative of a tumor nodule in the human lung. The calculations allow us to consider differences among the protocols in terms of several pharmacokinetic indices and in terms of the temporal and spatial distribution of antibody and antibody complexes in the tumor.

METHODS

Details of the models' formulations and limitations have been previously reported (*9–11*). Briefly, the models describe three physiological spaces: plasma, normal tissue interstitium and a densely cellular tumor nodule surrounded by normal tissue. The plasma concentrations are given by multiexponential equations that describe the decrease in concentration following bolus injection (Table 1). The multiexponential form implies distribution in other tissues in the body, but explicit volumes of distribution are not required. We assume that the plasma clearance of the MAb is unchanged by biotinylation or streptavidinylation. The equations for the normal tissue are ordinary differential equations which assume that the interstitial concentrations vary in time only.

For correspondence or reprints contact: Cynthia Sung, NIH, Building 13, Room 3N17, 9000 Rockville Pike, Bethesda, MD 20892-5766.

TABLE 1
Parameter Values

Plasma kinetics	Value	Footnote	Reference
MAb, MAb-sAv, MAb-b, MAb-sAv/biotin complex		*	11, 23
α_1	0.27		
α_2	0.73		
λ_1	$1.94\ 10^{-4}\ s^{-1}$		
λ_2	$7.43\ 10^{-6}\ s^{-1}$		
sAv		†	10
β_1	0.55		
β_2	0.45		
ξ_1	$3.03\ 10^{-4}\ s^{-1}$		
ξ_2	$1.35\ 10^{-5}\ s^{-1}$		
Biotin		‡	24
$\beta_1 0$	0.69		
β_2	0.24		
β_2	0.07		
ξ_1	$9.80\ 10^{-3}\ s^{-1}$		
ξ_2	$5.56\ 10^{-4}\ s^{-1}$		
ξ_3	$8.68\ 10^{-5}\ s^{-1}$		
MAb-b/sAv high mol. wt complex		§	10
η	$5.48\ 10^{-6}\ s^{-1}$		
Transport properties			
Lung transcapillary transport coefficient			
MAb, MAb-b	$4.6\ 10^{-5}\ s^{-1}$		10
MAb-sAv, MAb-sAv/biotin complex	$3.9\ 10^{-5}\ s^{-1}$	¶	
sAv	$1.0\ 10^{-4}\ s^{-1}$	**	15
biotin	$2.5\ 10^{-2}\ s^{-1}$	††	25
MAb-b/sAv high mol. wt complex	0		10
Lung volume efflux coefficient	$8.9\ 10^{-5}\ s^{-1}$	¶¶	10
Tumor effective diffusion coefficient			
MAb, MAb-b	$6.3\ 10^{-9}\ cm^2/s$		26
MAb-sAv, MAb-sAv/biotin complex, MAb-b/sAv complex	$4.2\ 10^{-9}\ cm^2/s$	‡‡, §§	
sAv	$1.8\ 10^{-8}\ cm^2/s$	‡‡	
Biotin	$4.6\ 10^{-6}\ cm^2/s$		11
Reaction parameters			
Rate constant for binding of MAb and antigen	$10^4\ M^{-1}\ s^{-1}$	¶¶	11
Rate constant for dissociation of MAb and antigen	$10^{-5}\ s^{-1}$	¶¶	11
Valence of MAb/antigen binding	2		
Antigen concentration	10^{-6} M	¶¶	27
Rate constant for binding of biotin and sAv	$7\ 10^7\ M^{-1}\ s^{-1}$		28
Rate constant for dissociation of biotin and sAv	$9\ 10^{-8}\ s^{-1}$		28
Valence of biotin binding to MAb-sAv	1	¶¶	See Methods
Valence of sAv binding to MAb-b	1	¶¶	10
Physiological properties			
Fractional hematocrit	0.42		
Interstitial volume fraction of lung	0.29		29
Interstitial volume fraction of tumor nodule	0.16	¶¶	27
Mean density of deflated lung	$1\ g/cm^3$	¶¶	

(Continued)

These equations describe transport across local blood capillaries, lymphatic efflux and the binding reactions that occur between the modified antibody (i.e., biotinylated or streptavidinylated MAb) and the second component.

An analysis of transcapillary protein transport by Rippe and Harraldson indicates that 75%–90% of albumin transport is due to convection through large pores, and that macromolecular solutes larger than albumin are essentially transported by convection only (*12*). Previously, we approximated the transcapillary transport of sAv (60 kDa) as a purely convective process (*10*). In the present work, we refine this treatment by ascribing 80% of transcapillary sAv transport to (unidirectional) convection through large pores and 20% to (bidirectional) diffusion through small pores (See Appendix). As before, we assume that transcapillary transport of the MAb species is entirely convective and that transport of radiolabeled biotin is bidirectional and symmetric (*10,11*). We note here the functional equivalence of our normal tissue equations and the treatment developed by Baxter et al. (*13*) for two-pore solute influx.

The equations for the tumor describe temporal and spatial variations in concentration; they incorporate diffusion in the tumor interstitium, binding and dissociation of antibody and antigen

TABLE 1
Parameter Values *(Continued)*

Plasma kinetics	Value	Footnote	Reference
Other parameters			
Radius of tumor nodule	150 μm		9
Rate constant for internalization of MAb-Ag complex			
No antigen turnover	0		
With antigen turnover	$1.16\ 10^{-5}\ s^{-1}$	¶¶	11
^{131}I decay rate	$10^{-6}\ s^{-1}$		

*For MAb, MAb-sAv, and MAb-b,

$$C_p(t) = C_{p0} \cdot \{\alpha_1 e^{-\lambda_1 t} + \alpha_2 e^{-\lambda_2 t}\}\ 0 \le t \le t_2;\ C_p(t) = 0 \quad t > t_2.$$

For MAb-sAv/biotin complex,

$$\overline{C^* C_p}(t) = C_p(t_2) \cdot \{\alpha_1 e^{-\lambda_1 t} + \alpha_2 e^{-\lambda_2 t}\}\ t > t_2;\ \overline{C^* C_p}(t) = 0 \quad 0 \le t \le t_2.$$

†For sAv,

$$\overline{C_p^*}(t) = C_{p0}^* \cdot \{\beta_1 e^{-\delta_1 (t-t_2)} + \beta_2 e^{-\delta_2 (t-t_2)}\}\ t > t_2;\ \overline{C_p^*}(t) = 0 \quad 0 \le t \le t_2.$$

In guinea pigs, the plasma clearance of sAv is 2.8 times higher than that of MAb (*10*). To approximate the plasma clearance of sAv in humans, the exponential rate constants from the guinea-pig equation were scaled so that the sAv clearance would be 2.8 times higher than the MAb clearance in humans.

‡For biotin,

$$\overline{C_p^*}(t) = C_{p0}^* \cdot \{\beta_1 e^{-\delta_1 (t-t_2)} + \beta_2 e^{-\delta_2 (t-t_2)} + \beta_3 e^{-\delta_3 (t-t_2)}\}\ t > t_2;\ \overline{C_p^*}(t) = 0 \quad 0 \le t \le t_2.$$

§For high molecular weight complexes of MAb-b and sAv,

$$\overline{C^* C_p}(t) = C_p(t_2) \cdot e^{-\pi t}\ t > t_2;\ \overline{C^* C_p}(t) = 0 \quad 0 \le t \le t_2.$$

In guinea pigs, the plasma half-life of MAb-b/sAv complex is 1.6 times shorter than the terminal half-life of MAb (*10*). To estimate the plasma half-life of complex in humans, we assumed that the same ratio would apply and accordingly scaled from the MAb value in humans.

¶Scaled from MAb value by the empirical molecular weight scaling relationship that capillary permeability of macromolecules varies as the inverse square root of molecular weight (*16*).

**Scaled from albumin values by the same molecular weight scaling relationship as above; albumin values estimated from data by Erdmann et al. (*15*) and from the assumption that 80% of transcapillary albumin transport is convective (*12*).

††Scaled from mannitol value by the molecular weight scaling relationship that capillary permeability of small, hydrophilic solutes is proportional to $(1/\text{mol wt})^{0.63}$ (*30*).

‡‡Scaled from MAb value by the empirical molecular weight scaling relationship that the effective diffusivity of macromolecules in tumors varies as $(1/\text{mol wt})^{1.14}$ (*31*).

§§The model simulations are not very sensitive to the value of diffusion coefficient of MAb-b/sAv complexes. For example, suppose that a high-molecular-weight (e.g., four-to-four) complex forms in the tissue. The diffusion coefficient would then be lowered 4.7-fold (*31*). In the high-dose case in the absence of antigen internalization, the peak average tumor concentration, the tumor-to-blood ratio at 24 hr, the tumor-to-lung ratio at 24 hr, the MRT, and the RE are 1.03, 1.07, 1.10, 1.20, and 1.38 times higher than the respective values for a one-to-one complex. Lower doses and antigen internalization produce even smaller perturbations.

¶¶Not measured experimentally but chosen as a representative value.

(Ag), and of the second component and the pretargeted antibody. We assume that binding of the various species in the tumor does not perturb the plasma kinetics. The model allows for internalization of MAb-Ag complexes. Internalization is treated as a first-order rate process that results in the immediate loss of the radionuclide bound to it and in the replacement of Ag at the cell surface. We examine the cases in which no internalization occurs and the internalization rate constant k_{met} equals $1.16\ 10^{-5}\ s^{-1}$ (corresponding to a time constant, $1/k_{met}$, of 24 hr). We have modeled an idealized radionuclide with a physical half-life of 8.07 days (as would be the case for ^{131}I) that deposits its energy at the point of localization. Absorbed energy distributions for actual nuclides can be calculated by methods described elsewhere (*14*), using the concentration profiles presented here as the source distributions.

Table 1 lists the values of the parameters used in these calculations. These parameters were taken from clinical data or were based on animal studies, with scaling, when necessary, for molecular weight or interspecies differences. Footnotes to Table 1 explain how plasma clearances of sAv and MAb-b/sAv complexes in humans were estimated from guinea pig data. The capillary permeability of MAb and lymphatic efflux coefficient in lung were determined from uptake and loss of MAb in guinea pig lungs (*8,10*). The lung capillary permeability of sAv was estimated from the steady-state plasma-to-lymph ratio of albumin in sheep lung (*15*). An adjustment for molecular weight was applied by multiplying the albumin permeability by the inverse square root of the molecular weight ratio (*16*). Permeability coefficients are similar in different mammalian species (*17*).

Calculations were performed for two different doses of antibody, corresponding to initial plasma concentrations of 50 n*M* and 200 n*M*. At the lower dose, the MAb concentration in the tumor nodule is below the concentration required to saturate the antigen; at the higher dose, saturating conditions prevail. These doses in a 70-kg human (3000 ml plasma volume) are approximately 23 mg and 90 mg of antibody, respectively. For the two-step protocols,

we considered a delay, t_2, of 72 hr between the injections of the modified antibody and of the second component, based on previous experimental and modeling experience with this time interval (*8,10,11*). With the values we have used in the plasma decay function, the MAb plasma concentration is 10.8% of its initial value after 72 hr. We assume that, upon injection of the second component, all residual circulating antibody must be fully saturated by the second component before a nonzero concentration of free second component can exist in the plasma. The initial free plasma concentration of sAv was chosen such that sAv would saturate the pretargeted antibody in the tumor between 9 and 10 hr after t_2. This choice reflects a compromise between obtaining faster tumor penetration by sAv than by MAb, and achieving adequate selectivity between tumor and normal tissues. Following 50 n*M* of MAb, an initial free plasma sAv concentration of 75 n*M* was required; following 200 n*M* of MAb, an initial free plasma sAv concentration of 105 n*M* was required. Calculations for the two-step protocol involving biotin used the same initial free plasma concentrations of the second component, 75 n*M* and 105 n*M*, following low and high doses of MAb-sAv, respectively.

At these concentrations of radiolabeled biotin, we assumed that endogenous biotin is not a significant source of competition for binding to MAb-sAv. We made this assumption because the plasma concentration of endogenous biotin and other avidin-binding substances is only 0.5–1.0 n*M* in humans (*18*). However, it is noteworthy that the plasma biotin concentration in rats is 10–15 n*M* and in rabbits is 6 n*M* (*19*). Therefore, endogenous biotin plays a more significant role in those species.

In previous modeling of the radiolabeled biotin protocol (*11*), we treated the binding of biotin by MAb-sAv as a trivalent reaction, assuming that one of the four biotin binding sites was consumed in the conjugation of sAv to MAb. However, the pharmacokinetic indices that represent ratios of quantities are relatively insensitive to the choice of valence. For the present study, we consider the reaction to be univalent, because it allows comparisons of the radiolabeled species on a similar molar concentration scale for all three protocols. As before, we suppose that MAb-b reacts with sAv in a one-to-one stoichiometry. We recognize that the radiolabeled biotin protocol may produce an amplification of molar concentration because of its multivalency, but note that it is also possible, by multiple labeling of antibody or sAv molecules, to achieve a similar degree of amplification in radionuclide concentration. Thus, univalency serves as a reasonable basis for comparison.

RESULTS

The high affinity binding interaction ($K_a = 10^9\ M^{-1}$) between antibody and tumor-associated antigen creates a "binding-site barrier" that retards diffusion of antibody through the tumor and produces a highly inhomogeneous MAb distribution (*9*). Antibody is initially localized near the surface of the tumor and diffuses slowly through the tumor as an advancing front. At the lower MAb dose (50 n*M* initial plasma concentration) in the absence of antigen turnover, the front reaches the center of the tumor (150 μ) after approximately 3 days. At the higher MAb dose (200 n*M* initial plasma concentration) in the absence of antigen turnover, the front reaches the nodule's center after approximately 16 hr. In our model, the rate of penetration of MAb-b is the same as that of native antibody, because biotinylation is assumed to have no effect on either the plasma kinetics or the rates of antibody permeation and diffusion. MAb-sAv, however, with a molecular weight 40% greater than that of native MAb, is expected to have a lower capillary permeability and interstitial diffusivity than MAb (Table 1). As a result, at the low dose, approximately 9 days are required for MAb-sAv to reach the center of the tumor nodule; at the high dose, approximately 28 hr are required. If the initial plasma concentration is increased to 350 n*M*, the concentration profiles of MAb-sAv in the tumor develop at a rate similar to that of native or biotinylated MAb at 200 n*M* initial plasma concentration.

Panel A of Figure 1 shows the spatial distribution of directly radiolabeled MAb at the high dose in the absence of antigen turnover. Before the MAb reaches the center of the tumor nodule, the concentration profiles exhibit a sharp gradient: a drop from an antigen-saturating concentration to zero occurs over 30–40 μm. In the two-step protocols, the distribution of the first component (the biotinylated or streptavidinylated MAb) serves as the binding site distribution for the radiolabeled second component. At the high dose and in the absence of antigen turnover, the concentration of modified MAb is predicted to be uniform across the tumor 72 hr after injection. The distribution of total sAv after pretargeting with MAb-b is illustrated in Panel B of Figure 1. The gradient of sAv concentration is narrower than the gradient of MAb observed in Panel A because the affinity between sAv and the MAb-b ($K_a \sim 10^{15}\ M^{-1}$) is much greater than the affinity between antibody and antigen ($K_a = 10^9\ M^1$). The dose of sAv (corresponding to an initial free plasma concentration of 105 n*M*) was chosen such that it would reach saturating concentrations in the center of the nodule 9–10 hr after administration. At the same initial free plasma concentration, biotin rapidly saturates the MAb-sAv that is uniformly distributed throughout the tumor (Panel C). Within 1 hr of administration (the first time interval for which the solutions to these equations are plotted), biotin has diffused to the center of the tumor nodule and saturated the MAb-sAv there. Model calculations indicate that a considerably lower dose of biotin (approximately 20 n*M* initial free biotin concentration in the plasma) would suffice to achieve such rapid saturation of the MAb-sAv at the tumor center.

Tumor-to-blood and tumor-to-lung ratios are plotted in Figure 2. Panels A through D correspond to the case in which no antigen turnover occurs. The data are plotted as a function of time *after injection of the radionuclide* (i.e., radiolabeled MAb in the one-step delivery, and radiolabeled sAv or radiolabeled biotin in the two-step protocols). The two-step protocol involving radiolabeled biotin produces considerably higher tumor-to-blood and tumor-to-lung ratios than does one-step MAb delivery: six- to eightfold higher at 24 hr for both the low and high doses. The degree of enhancement is even greater at earlier times. At the low dose, the two-step protocol involving radiolabeled sAv produces a tumor-to-blood ratio at 24 hr that is 40% higher than in the one-step protocol, and the tumor-to-lung

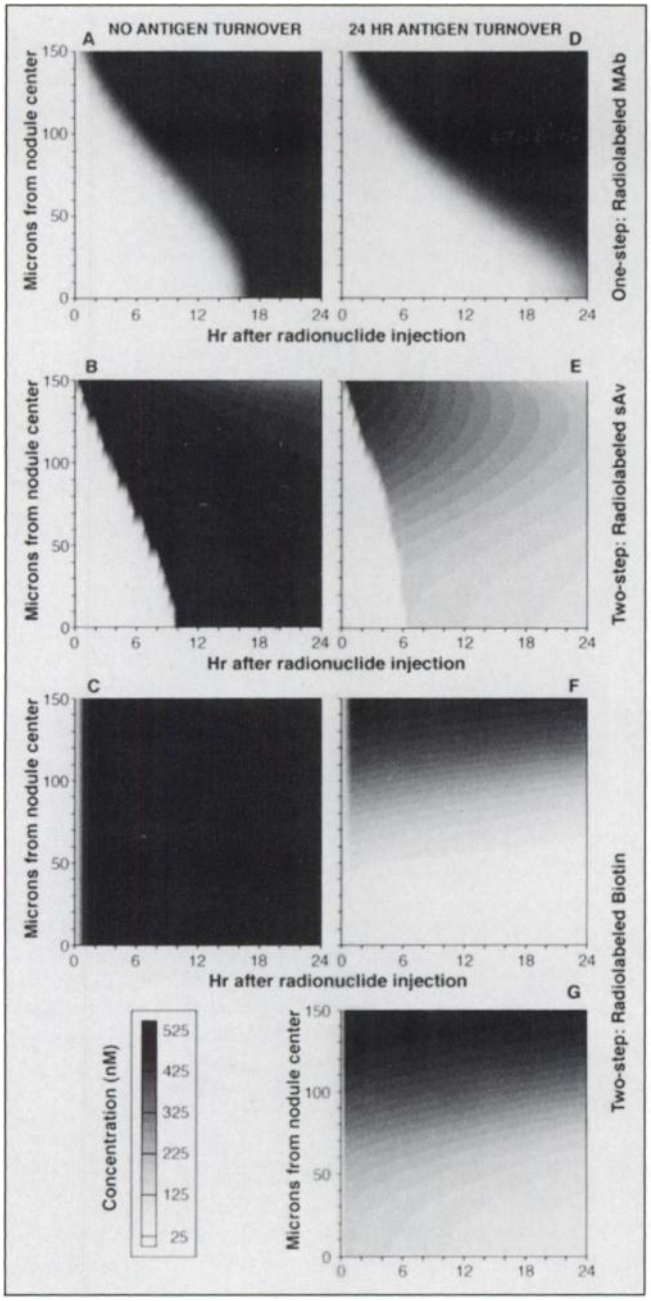

FIGURE 1. Temporal development of spatial distribution in a 150-μm radius tumor nodule of MAb in a one-step protocol (A and D); of sAv following pretargeting by MAb-b (B and E); and of biotin following pretargeting by MAb-sAv (C, F and G). Panels A to C represent the case in which no internalization of antibody-antigen complexes occurs; panels D to G represent the case in which internalization occurs with a 24-hr time constant. The initial free plasma concentration of MAb, MAb-b, or MAb-sAv is 200 nM in panels A to F, and 350 nM in panel G. The initial free plasma concentration of the second component in the two-step protocols (radiolabeled sAv or radiolabeled biotin) is 105 nM (panels B, C, E, F and G).

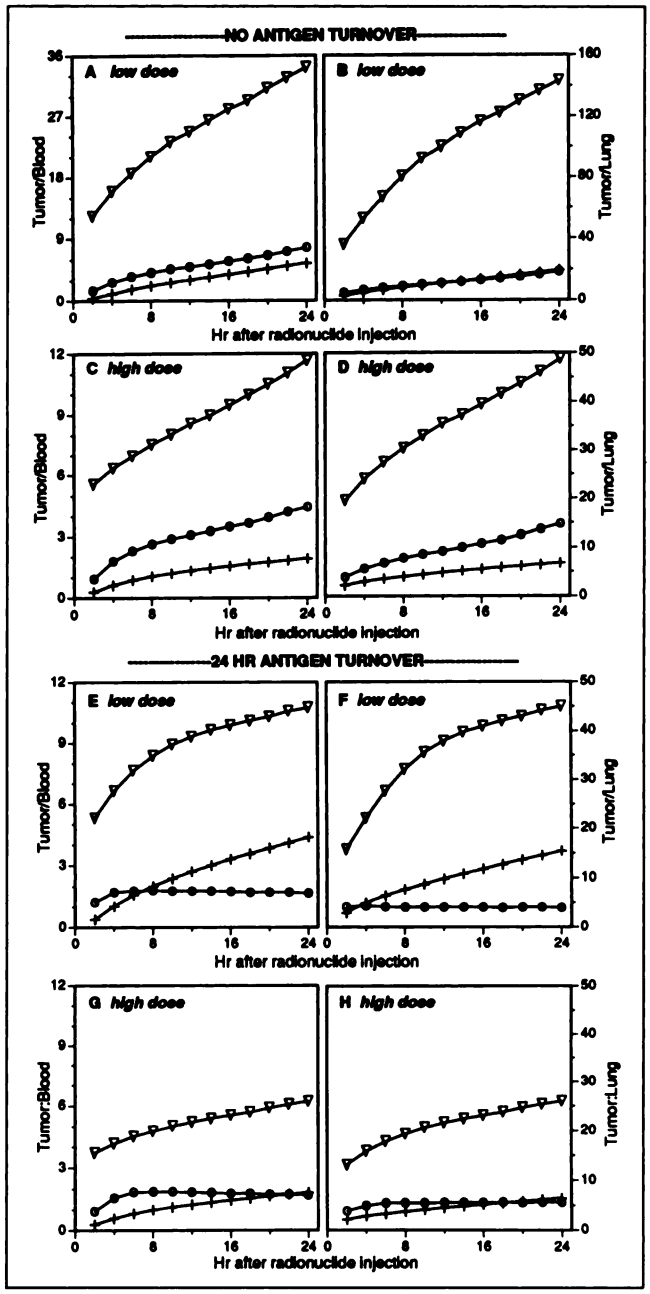

FIGURE 2. Calculated tumor-to-blood (A, C, E, G) and tumor-to-lung (B, D, F, H) ratios obtained following injection of radiolabeled MAb in a one-step protocol, -+-; following injection of radiolabeled sAv after pretargeting with MAb-b, -⊖-; and following injection of radiolabeled biotin after pretargeting with MAb-sAv, -▽-. Ratios are shown at low dose (A, B, E, F) and at high dose (C, D, G, H).

ratios are nearly the same. At the high dose, tumor-to-blood and tumor-to-lung ratios at 24 hr are 2.3- and 2.2-fold higher, respectively, than the values obtained from one-step MAb delivery. The high dose results are similar to model predictions and experimental results obtained in the guinea pig (*8,10*). This degree of enhancement in tumor-to-blood ratios is similar to that obtained with the use of $F(ab')_2$ fragments (*20*).

Another way of comparing the one- and two-step protocols is to consider the time required to achieve a particular tumor-to-blood or tumor-to-lung ratio. For example, at the high dose of MAb, a tumor-to-blood ratio of 10 is attained 90 hr after injection of directly labeled MAb; 52 hr after injection of radiolabeled sAv (124 hr after injection of

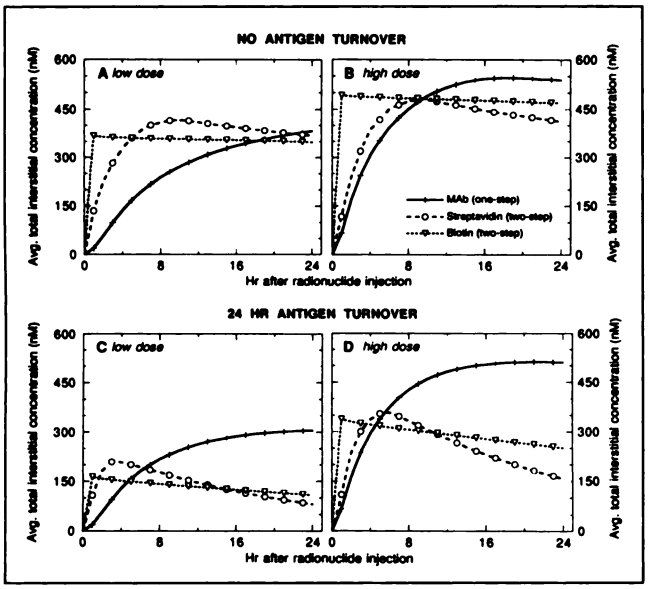

FIGURE 3. The average total molar concentration of MAb, sAv, or biotin in the tumor interstitium, both in the absence of internalization of antibody-antigen complexes (A and B) and in the presence of antigen turnover (C and D), at low dose (A and C) and at high dose (B and D). In A and C, the peak MAb concentration occurs after the 24-hr period shown here; in A the peak concentration is 430 nM at 64 hr, and in C it is 306 nM at 26 hr. The radioactivity per g of tumor can be calculated by multiplying the molar concentration by the molar specific activity of the radiolabeled species and the interstitial volume fraction.

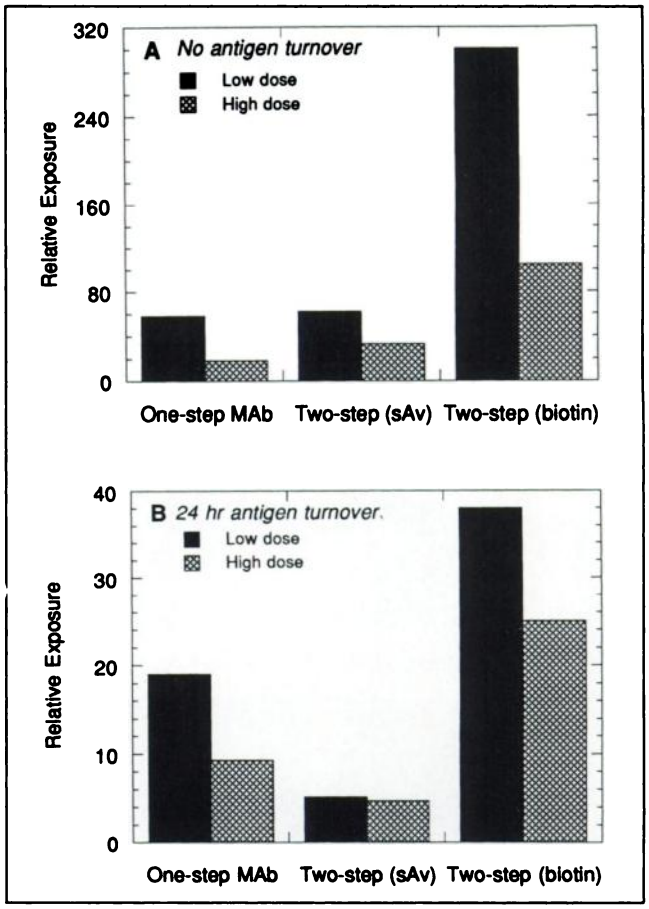

FIGURE 4. The relative exposures for the one-step and two-step protocols at both low dose and high dose. The calculations model a radionuclide that decays with a rate constant of 10^{-6} s^{-1} (e.g., ^{131}I). (A) Calculations for which no internalization of antibody-antigen complexes occurs. (B) Internalization that occurs with a time constant of 24 hr.

MAb-b); and 18 hr after injection of radiolabeled biotin (90 hr after injection of MAb-sAv). Thus, the time interval between injection of the *radiolabeled* species and the attainment of a particular tumor-to-blood ratio is shortened by the use of a two-step protocol, but the time of the entire procedure (the time after injection of the MAb or modified MAb) is not.

Enhancement of tumor-to-nontumor ratios is not sufficient to judge the superiority of a protocol. The radioactivity that each protocol produces in the tumor nodule is also crucially important. The graphs in panels A and B of Figure 3 indicate that, for both the low- and high-dose regimens in the absence of antigen turnover, the three protocols produce roughly equal maximal total *molar* concentrations of MAb, sAv or biotin in the tumor interstitium. In order to achieve comparable *radioactivity* in the pretargeting protocols as in one-step MAb targeting, the molar specific activity of the radiolabeled second component must be comparable to that of the radiolabeled antibody (or at least within a factor of three, if biotin binding is trivalent). For example, in the two-step protocol involving radiolabeled biotin, the biotin derivative should be labeled at a molar specific activity on the order of magnitude of 100 mCi/μmole if the corresponding directly-labeled antibody has a mass specific activity of 1 mCi/mg. Figure 3 also illustrates that the peak concentration is reached sooner in the two-step protocols than in the one-step method; the peak biotin concentration is achieved by the first timepoint of our calculations (1 hr).

The relative exposure (RE) is defined as the ratio of the area under the concentration curve (AUC) of the radiolabeled species in the tumor (including the rate of radionuclide decay) and the corresponding AUC in plasma (*11*). Its calculation includes the contribution from complexes formed in the plasma between the second component and modified MAb still circulating at time t_2. However, it ignores biochemical mechanisms by which loss of radiolabel can occur such as dehalogenation or interstitial proteolysis, and thus, the predicted value of RE may be higher than is attainable experimentally. Nonetheless, the qualitative comparison among the different protocols is informative. RE values for the different protocols in the absence of antigen turnover are shown in Figure 4A. At both low and high doses, the RE obtained with the two-step protocol involving radiolabeled biotin is approximately 5 to 6 times higher than the value achieved by one-step delivery, due principally to a reduction in plasma AUC. At the low dose, the two-step protocol involving radiolabeled sAv achieves

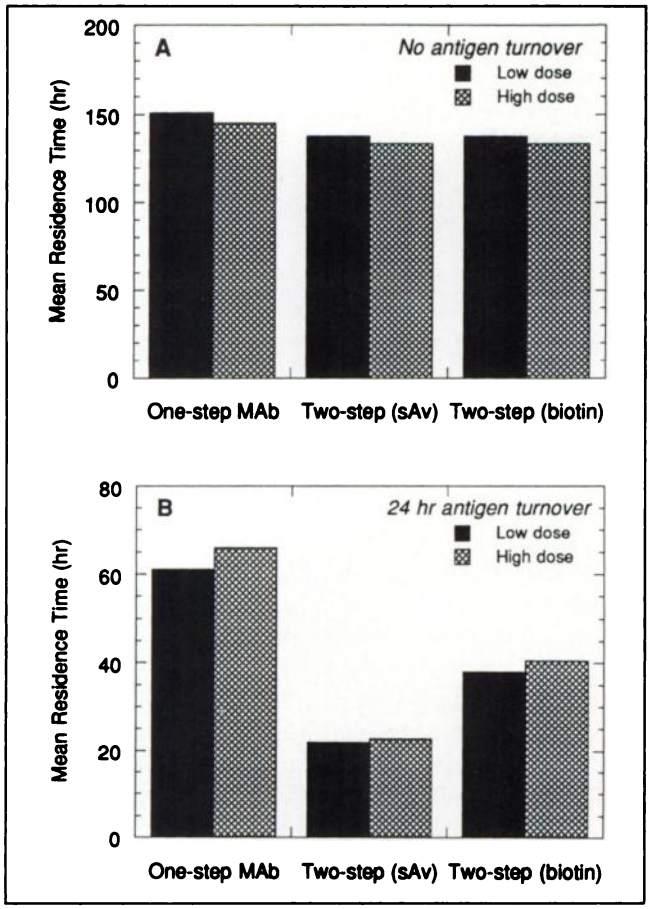

FIGURE 5. The mean residence times for the one-step and two-step protocols at both low dose and high dose. The calculations model a radionuclide that decays with a rate constant of 10^{-6} s^{-1} (e.g., ^{131}I). (A) calculations for which no internalization of antibody-antigen complexes occurs. (B) Internalization that occurs with a time constant of 24 hr.

an RE approximately equal to that achieved by one-step MAb delivery because the plasma AUC and the tumor AUC are both reduced by approximately the same factor relative to the corresponding values in the one-step protocol. At the high dose, the value of RE for radiolabeled sAv is 1.7 times the value for radiolabeled MAb, largely due to a lower plasma AUC. In simulations of guinea pig experiments carried out at approximately double the initial plasma concentration of MAb and radiolabeled sAv, we calculated an enhancement in RE of 2.2 (*10*). These calculations indicate that the enhancement in RE of the radiolabeled sAv protocol relative to one-step MAb delivery is very sensitive to the doses used.

The mean residence time (MRT), defined as the area under the moment (concentration · time) curve normalized by the AUC for the radiolabeled species, is a measure of the average length of time that radionuclide is retained in the tumor nodule. As illustrated in Figure 5A, in the absence of antigen internalization, only slight differences in the MRT are found among the different protocols, regardless of the dose regimen. This result is obtained because the principal determinant of the MRT of the radionuclide is the MRT of the antibody, which is similar in all three protocols.

Effects of Internalization of MAb-Ag Complexes

The dynamics of antigen turnover can vary considerably, depending upon the antibody and the antigen. For these calculations, we assumed that the rate at which antibody-antigen complex is internalized matches the rate at which antigen reappears on the surface of the tumor cell; thus, a steady-state antigen surface concentration is maintained. The continual presentation of new antigen to antibody diffusing through the tumor reduces the concentration of free antibody in the tumor interstitium. As a result, diffusion of MAb to the center of the tumor nodule is slowed (compare Fig. 1, panels A and D). Our treatment also includes rapid degradation of internalized antibody, with immediate loss of radionuclide from the cell (approximating the processing of ^{131}I, but not accurate for ^{111}In or ^{90}Y). Internalization thus lowers the average tumor concentration of antibody (and of radiolabel in one-step delivery). Consequently, the concentration of binding sites for the second component is reduced. Panels E and F of Figure 1 illustrate the impact of internalization on the distribution of the radiolabeled second component in the tumor. The effect is quite pronounced in these examples, because a t_2 of 72 hr is considerably longer than the characteristic turnover time constant. Thus, in the face of significant antigen turnover, the choice of t_2 can be critically important to the success of a protocol.

Antigen turnover can also lead to significant spatial gradients in the concentration of the radiolabeled species. For example, in Figure 1F, the initial plasma concentration of MAb-sAv (200 n*M*) is insufficient to reach the center of the tumor nodule. Hence, when radiolabeled biotin is administered, virtually none accumulates at the nodule's center because of the absence of binding sites (i.e., MAb-sAv) there. However, because the dose of MAb-sAv is approaching that required to saturate the antigen, the profiles are extremely sensitive to the dose of MAb-sAv in this range. If the initial plasma concentration is increased from 200 n*M* to 350 n*M* and all other parameters are kept constant, a substantial concentration of biotin (160 n*M*) is obtained at the center of the nodule 0.5 hr after t_2 (Fig. 1G). Under these conditions, the tumor-to-blood and tumor-to-lung ratios at 24 hr after t_2 are still higher (by factors of 2.5 and 3, respectively) than the corresponding ratios for the one-step MAb delivery.

Antigen turnover lowers the tumor-to-blood and tumor-to-lung ratios in all of the protocols, as can be seen by comparing panels A through D with panels E through H in Figure 2. The two-step protocol involving radiolabeled biotin still produces higher ratios than one-step MAb delivery at equivalent times after radionuclide injection; however, the relative improvement is lower than in the absence of internalization. At the higher dose, the tumor-to-blood and tumor-to-lung ratios are 3.4- and 4-fold higher, respec-

tively, than the corresponding ratios for the one-step MAb protocol at 24 hr. At early times after injection of radiolabeled sAv, a small degree of enhancement in the ratios is predicted relative to the values achieved with one-step MAb delivery; but this enhancement declines with time, and the protocol at later times produces ratios lower than those obtained with direct MAb targeting.

For all three protocols, the average concentration of the radiolabeled species in the tumor interstitium is reduced by antigen turnover, as illustrated in panels C and D of Figure 3. But the two-step protocols are more strongly affected, due to the long t_2 (72 hr) compared to the characteristic turnover time (24 hr). The peak concentrations are reduced by 30%–50%, and the rates at which radionuclide is lost from the tumor nodule are somewhat faster. In the radiolabeled biotin protocol, the RE is still approximately 2–3 times higher than the RE for the one-step MAb method (Fig. 4B). The RE obtained with radiolabeled sAv is lower than that obtained with one-step MAb delivery. Figure 5B indicates that antigen turnover reduces the MRT obtained in all three protocols, with a two- to three-fold greater effect in the two-step protocols. The MRT is less severely degraded if radiolabeled biotin rather than radiolabeled sAv is the second component.

DISCUSSION

Pharmacokinetic considerations support the further investigation and development of the two-step MAb-based targeting protocol utilizing radiolabeled biotin as the second component. At the low and high doses in the absence of antigen turnover, the models predict that the time after injection of the radionuclide required to attain a desired tumor-to-blood or tumor-to-lung ratio is shorter in comparison with directly-labeled MAb. The maximal molar concentration of radiolabeled species in the tumor is comparable in all three protocols but is attained much faster with the radiolabeled biotin protocol. Consequently, the use of short-lived radioisotopes like ^{99m}Tc, with a 6-hr half-life, becomes feasible. The models also predict that the biotin protocol yields higher REs and comparable MRTs, favorable indications for therapeutic applications.

Internalization and degradation of antibody-antigen complexes negatively affect all of the tumor-targeting protocols; for the cases we have modeled, nevertheless, the two-step protocol involving radiolabeled biotin still produces the highest values of tumor-to-blood and tumor-to-lung ratios and of RE. However, the maximal tumor concentration and MRT obtained in the radiolabeled biotin protocol are lower than those obtained in direct MAb targeting, and the radionuclide is less homogeneously distributed in the tumor. Thus, in the presence of antigen turnover, tradeoffs in peak concentration, spatial distribution and MRT accompany the higher tumor-to-blood and tumor-to-lung ratios and REs of the two-step biotin protocol. The particular application will determine whether these tradeoffs are acceptable. Adjustments to the protocol, such as increasing the dose of MAb-sAv, can improve the average tumor concentration, spatial distribution and MRT but will lower the tumor-to-nontumor ratios. However, within a limited range, it is still possible to achieve higher ratios than can be obtained with the one-step protocol. Alternatively, it may be possible to target an antigen with slower internalization kinetics.

If radiolabeled biotin is not sequestered in nontarget organs, the higher RE in the two-step protocol would be expected to produce lower toxicity, thus permitting the use of higher doses or more frequent dosing. Support for the lack of biotin sequestration in normal tissues is suggested by experimental data in dogs, which show that greater than 80% of an injected dose of ^{111}In-DTPA-biotin is excreted in the urine within 6 hr (*21*). From biodistribution data in that report, we estimate that 6% of the injected dose is in the kidneys at 6 hr. Moreover, data from normal rats show that only 3% of an injected dose of ^{14}C-labeled biotin accumulates in the liver (*22*).

Evaluation of the two-step protocol involving radiolabeled sAv yields a much more equivocal picture of the pharmacokinetic advantage of this approach. Any advantage appears much more dependent on dose, on the degree of antigen turnover, and on the time after administration of radiolabel at which this protocol is compared to one-step delivery. Our conclusions regarding the favorable pharmacokinetic advantage of the radiolabeled biotin protocol are more robust than those concerning the radiolabeled sAv protocol, because the capillary permeability and interstitial diffusivity of biotin are three orders of magnitude higher than those of directly radiolabeled MAb. These transport parameters for sAv, on the other hand, are only 2–3 times higher than those of MAb.

The pharmacokinetic models provide some guidance in the design of a clinical trial of the two-step targeting protocol involving radiolabeled biotin. To take maximum advantage of the specific targeting of MAb-sAv, the dose of biotin should saturate the MAb-sAv that localized in the tumor during the first step (*11*). The dose of biotin required to saturate the MAb-sAv can be estimated from biodistribution data of the MAb-sAv and, in the case of extensive disease, from the antigen burden. Because transport and clearance occur much more rapidly for free biotin than for MAb-sAv/biotin complex, a dose of biotin several times higher than the just-saturating dose does not substantially reduce the tumor-to-nontumor ratios. Thus, there is considerable latitude in the dose of radiolabeled biotin once the saturation condition has been met. Our calculations indicate that the pharmacokinetic indices are determined almost entirely by the amounts of MAb-sAv in the plasma, in normal tissues, and in the tumor at the time of injection of radiolabeled biotin. Dose escalation should therefore focus on MAb-sAv because of its dominant role in controlling the distribution and penetration of the radiolabeled biotin. Monitoring the pharmacokinetics of MAb-sAv would be a desirable element of the protocol, especially if MAb-sAv

clearance varied considerably from patient to patient or from treatment to treatment.

In our simulations of the two-step protocols, we find that the complexes which form in the plasma between the modified MAb and the radiolabeled second component contribute to a high percentage of the plasma radioactivity. It has been shown experimentally that the use of an intermediate clearing step, in which the concentration of modified MAb is lowered prior to administration of the radiolabeled species, eliminates this source of plasma radioactivity and enhances the tumor-to-blood ratio (*1*). Although we have not modeled the application of a clearing step here, we previously described an approximate treatment of this process for the radiolabeled sAv protocol (*10*). A similar treatment could be developed for the radiolabeled biotin protocol. The models then could be used to calculate the effect of such a step on the other pharmacokinetic indices.

The models presented here can be further extended to incorporate the energy distributions and cellular processing of specific radionuclides. This treatment would permit the calculation of the spatial and temporal radiation dose distributions within a tumor nodule, and it might prove to be helpful in identifying the optimal radionuclide in a particular two-step targeting protocol.

CONCLUSION

The two-step protocol involving radiolabeled biotin given after pretargeting with streptavidinylated MAb produces enhancements in many important pharmacokinetic ratios relative to those obtained with directly radiolabeled MAb. The degree of enhancement depends on a number of experimentally controllable variables. The pharmacokinetic models can guide in the selection of those variables and thereby facilitate optimization of the protocol.

APPENDIX

The equation below describes the normal tissue concentration of free sAv, $C_e^*(t)$. It is a function of the transcapillary transport coefficient (κ^*), the volume efflux coefficient (Λ), the fraction of transcapillary transport due to symmetric, bidirectional transport (f), and the forward and reverse rate constants of the binding reaction between MAb-b and sAv (k_f^* and k_r^*, respectively). The plasma concentration of free sAv and the normal tissue concentrations of free MAb-b and of the MAb-b/sAv complex are denoted by $C_p^*(t)$, $C_e(t)$, and $\overline{C * C}_e$, respectively. $f \cdot \kappa^*$ is the contribution of diffusion through small pores to total solute transport and $(1 - f) \cdot \kappa^*$ is the contribution of convection through large pores. Hence, the first term on the right side of the equation represents the sum of diffusive and convective processes of transcapillary solute influx.

$$\frac{dC_e^*(t)}{dt} = \kappa^* \cdot C_p^*(t) - (\Lambda + f \cdot \kappa^*) \cdot C_e^*(t)$$

$$- k_f^* \cdot C_e(t) \cdot C_e^*(t) + k_r^* \cdot \overline{C * C}_e(t)$$

ACKNOWLEDGMENTS

The authors thank Drs. Robert L. Dedrick, John N. Weinstein, Ronald D. Neumann and Tsuneo Saga for helpful and stimulating discussions on this subject and Barry Bowman for careful editing of the manuscript. We would also like to acknowledge the Advanced Scientific Computing Laboratory of the Frederick Cancer Research Facility of the National Cancer Institute for allocation of computing time and staff support.

REFERENCES

1. Goodwin DA, Meares CF, McCall MJ, McTigue M, Chaovapong W. Pretargeted immunoscintigraphy of murine tumors with indium-111-labeled bifunctional haptens. *J Nucl Med* 1988;29:226–234.
2. Paganelli G, Riva P, Deleide G, et al. In vivo labeling of biotinylated monoclonal antibodies by radioactive avidin: a strategy to increase tumor radiolocalization. *Int J Cancer* 1988;2(suppl):121–125.
3. Pimm MV, Fells HF, Perkins AC, Baldwin RW. Iodine-131 and indium-111 labeled avidin and streptavidin for pretargeted immunoscintigraphy with biotinylated and anti-tumor monoclonal antibody. *Nucl Med Commun* 1988; 9:931–941.
4. LeDoussal JM, Martin M, Gautherot E, Delaage M, Barbet J. In vitro and in vivo targeting of radiolabeled monovalent and divalent haptens with dual specificity monoclonal antibody conjugates: enhanced divalent hapten affinity for cell bound antibody conjugate. *J Nucl Med* 1989;30:1358–1366.
5. Kalofonos HP, Rusckowski M, Lavendar JP, Epenetos AA, Hnatowich DJ. Radioimmunotargeting of tumor in patients with streptavidin and biotin [Abstract]. *J Nucl Med* 1989;30:819.
6. Stickney DR, Anderson LD, Slater JB, et al. Bifunctional antibody: a binary radiopharmaceutical delivery system for imaging colorectal carcinoma. *Cancer Res* 1991;51:6650–6655.
7. Khawli LA, Alauddin MM, Miller GK, Epstein AL. Improved immunotargeting of tumors with biotinylated monoclonal antibodies and radiolabeled streptavidin. *Antibod Immunoconj Radiopharm* 1993;6:13–27.
8. Saga T, Weinstein JN, Jeong JM, et al. Two-step targeting of experimental lung metastases with biotinylated antibody and radiolabeled streptavidin. *Cancer Res* 1994;54:2160–2165.
9. van Osdol WW, Fujimori K, Weinstein JN. An analysis of monoclonal antibody distribution in microscopic tumor nodules: consequences of a "binding site barrier." *Cancer Res* 1991;51:4776–4784.
10. Sung C, van Osdol WW, Saga T, Neumann RD, Dedrick RL, Weinstein JN. Streptavidin distribution in metastatic tumors pretargeted with a biotinylated monoclonal antibody: theoretical and experimental pharmacokinetics. *Cancer Res* 1994;54:2166–2175.
11. van Osdol WW, Sung C, Dedrick RL, Weinstein JN. A distributed pharmacokinetic model of two-step imaging and treatment protocols: application to streptavidin conjugated monoclonal antibodies and radiolabeled biotin. *J Nucl Med* 1993;34:1552–1564.
12. Rippe B, Haraldsson B. Fluid and protein fluxes across small and large pores in the microvasculature. Application of two-pore equations. *Acta Physiol Scand* 1987;131:411–428.
13. Baxter LT, Zhu H, Mackensen DG, Jain RK. Physiologically based pharmacokinetic model for specific and nonspecific monoclonal antibodies and fragments in normal tissues and human tumor xenografts in nude mice. *Cancer Res* 1994;54:1517–1528.
14. Fujimori K, Fisher DR, Weinstein JN. Integrated microscopic-macroscopic pharmacology of monoclonal antibody radioconjugates: the radiation dose distribution. *Cancer Res* 1991;51:4821–4827.
15. Erdmann J III, Vaughan TR Jr, Brigham KL, Woolverton WC, Staub NC. Effect of increased vascular pressure on lung fluid balance in unanesthetized sheep. *Circulation Res* 1975;37:271–284.
16. Peterson HI, Applegren L, Lundborg G, Rosengren B. Capillary permeability of two transplantable rat tumours as compared with various normal organs of the rat. *Bibl Anat* 1972;12:511–518.
17. Renkin EM. Multiple pathways of capillary permeability. *Circ Res* 1977;41: 735–743.
18. Mock DM, Malik MI. Distribution of biotin in human plasma: most of the biotin is not bound to protein. *Am J Clin Nutr* 1992;56:427–432.
19. Mock DM. Evidence for a pathogenic role of ω6 polyunsaturated fatty acid in the cutaneous manifestations of biotin deficiency. *J Ped Gastro Nutr* 1990;1990:222–229.
20. Buchegger F, Haskell CM, Schreyer M, et al. Radiolabeled fragments of monoclonal antibodies against carcinoembryonic antigen for localization of

human colon carcinoma grafted into nude mice. *J Exp Med* 1983;158:413–427.
21. Rosebrough SF. Pharmacokinetics and biodistribution of radiolabeled avidin, streptavidin, and biotin. *Nucl Med Biol* 1993;20:663–668.
22. Petrelli F, Moretti P, Paparelli M. Intracellular distribution of biotin-^{14}COOH in rat liver. *Molec Biol Rep* 1978;4:247–252.
23. Eger RR, Covell DG, Carrasquillo JA, et al. Kinetic model for the biodistribution of an ^{111}In-labeled monoclonal antibody in humans. *Cancer Res* 1987;47:3328–3336.
24. Houston AS, Sampson WFD, Macleod MA. A compartmental model for the distribution of ^{113m}In-DTPA and ^{99m}Tc-(Sn)DTPA in man following intravenous injection. *Inter J Nucl Med Biol* 1979;6:85–95.
25. Brigham KL, Harris TR, Rowlett RD, Owen PJ. Comparisons of [^{14}C]urea and [^{3}H]mannitol as lung vascular permeability indicators in awake sheep: evidence against red cell urea trapping. *Microvasc Res* 1977;13:97–105.
26. Clauss MA, Jain RK. Interstitial transport of rabbit and sheep antibodies in normal and neoplastic tissues. *Cancer Res* 1990;50:3487–3492.
27. Fujimori K, Covell DG, Fletcher JE, Weinstein JN. Modeling analysis of the global and microscopic distribution of immunoglobulin G, F(ab')$_2$, and Fab in tumors. *Cancer Res* 1989;49:5656–5663.
28. Green NM. Avidin: 1. The use of [^{14}C]biotin for kinetic studies and for assay. *Biochem J* 1963;89:585–591.
29. Jain RK. Transport of molecules in the tumor interstitium: a review. *Cancer Res* 1987;47:3039–3051.
30. Dedrick RL, Flessner MF, Collins JM, Schultz JS. Is the peritoneum a membrane? *ASAIO J* 1982;5:1–8.
31. Nugent LJ, Jain RK. Extravascular diffusion in normal and neoplastic tissue. *Cancer Res* 1984;44:238–244.

EDITORIAL

Tumor Pretargeting: Almost the Bottom Line

Human imaging studies have shown that while maximum human tumor concentrations of MAb are achieved in one day, the slow pharmacokinetics requires several days for the background to fall sufficiently for sensitive radioimmunoscintigraphy of tumors. With therapeutic radionuclides such as ^{90}Y, this long biological half-life imposes a high radiation burden on sensitive normal tissues from the large amount of retained radioactivity. Normal tissue toxicity, especially to the bone marrow, has been the major limiting factor in the application of radioimmunotherapy to solid tumors. The use of improved bifunctional chelating reagents and techniques reduces free yttrium, lowers liver, bone and marrow uptake and decreases the radiation dose to these normal organs. Pretargeting techniques provide an alternative way to get high selective tumor uptake of ^{90}Y with simultaneous minimization of nontarget tissue background.

Pretargeting involves administration of a long-circulating targeting macromolecule (MAb) having a high affinity noncovalent binding site for a small rapidly excreted effector molecule, which is given after the MAb has concentrated in the target tumor (T). Removal of the macromolecule-binder conjugate from the circulation with a polyvalent "chase" macromolecule before giving the effector molecule greatly improves the target-to-blood ratio (T/B). The aggregated MAb produced by cross-linking with the chase in the circulation, is rapidly endocytosed by reticuloenothelial cells (Kupffer cells), mostly in the liver (*1*). The intracellular location of the endocytosed MAb prevents the access and binding of subsequently injected effector molecules, so liver uptake of radioactivity remains low. Soon, (approximately 1 hr) after the chase, the effector molecule (radiolabeled hapten or biotin conjugate) is given, and the maximum tumor concentration and tumor- to-normal tissue ratio is achieved in 1–3 hr. Unbound radiolabel (> 90% of the injected dose) is rapidly excreted via the kidneys, leading to greatly decreased radiation exposure to normal tissues. Several targeting macromolecule-conjugate / effector small molecule pairs have been proposed (Table 1 and Fig. 1). Examples are: MAb/hapten (*2–5*), MAb-avidin/biotin (*6*), MAb-biotin/avidin (*7*), MAb-enzyme/prodrug (*8,9*) and MAb-oligonucleotide/antisense oligonucleotide (*10*). These systems give higher target-to- normal tissue ratios with less toxicity than covalent conjugates of MAbs and effector molecules.

Qualitative comparison of the pharmacokinetics of directly labeled MAb, two-step and three-step pretargeting is depicted in Figures 2, 3 and 4. For simplicity, only the blood and tumor concentrations are illustrated over 4 days. Directly labeled MAb circulates for days with maximum tumor concentration occurring at 1–2 days with continuing high blood concentration for several more days (Fig. 2). Reducing the circulating half-time by decreasing the molecular size [F(Ab), F(v) fragments, peptides] improves the tumor-to-blood ratio, but decreases the time integral in the blood (blood concentration × time). This shortens the period during which a high concentration gradient exists between the blood and the tumor, which is the driving force for diffusion into the tumor. In addition, high concentrations in nontarget normal organs such as the kidney [Fab] (*11*) and lung [VIP] (*12*) can be problematic with labeled fragments and peptides (*13*). Thus, with directly labeled low molecular weight fragments, a low blood concentration giving high T/B1 ratios is achieved only at the cost of lower tumor uptake.

Pretargeting combines the pharmacokinetics of long circulating MAb with rapidly excreted small effector molecules to give both high tumor concentration and high tumor-to-normal tissue ratios (Figs. 3 and 4). The two-step method eliminates radiation during the MAb localizing phase, which can take several days. Nonspecific localization at this stage in liver, spleen and bone marrow, due to damaged or heavily labeled molecules and aggregates, does not contribute to normal tissue radiation since radioactivity is only injected later. Previous at-

Received Feb. 6, 1995; accepted Feb. 7, 1995.
For correspondence or reprints contact: David A. Goodwin, MD, Professor of Radiology, Stanford University School of Medicine, Chief of Nuclear Medicine, Veterans Administration Medical Center, 3801 Miranda Ave., Palo Alto, CA 94304.